Nuclear Inst. and Methods in Physics Research, A 869 (2017) 56–62

Contents lists available at ScienceDirect

Nuclear Inst. and Methods in Physics Research, A

journal homepage: www.elsevier.com/locate/nima

Design and optimisation of the positron production chain for CLIC from the target to the damping ring

C. Bayar [a,b,*], A.K. Ciftci [a,c], S. Doebert [b], A. Latina [b]

[a] Ankara University, Ankara, Turkey
[b] CERN, Geneva, Switzerland
[c] Izmir University of Economics, Izmir, Turkey

ARTICLE INFO

Keywords:
Positron source
Linac
Tracking
Optimisation
Design
Decelerating mode

ABSTRACT

The CLIC Positron source has been designed to produce non-polarised positron beams using a hybrid target composed of a crystal followed by an amorphous target. After production, positrons are captured and accelerated to 200 MeV in the pre-injector linac and subsequently accelerated further up to 2.86 GeV in the injector linac. At this point they enter the pre-damping ring and afterwards the main damping ring to obtain the necessary beam quality for a linear collider. In this study, we have designed and optimised the beam transport and acceleration from the target to the pre-damping ring which has a limiting transverse and longitudinal acceptance. The goal of the study was to maximise the positron yield accepted by the pre-damping ring.

Contents

1. Introduction

The positron source for CLIC needs to deliver intense high quality positron beams for the linear collider. Depending on the construction stage of the collider the source needs to deliver trains of up to 352 bunches with a bunch repetition rate of 2 GHz and up to 5.2×10^9 positrons per bunch to the main linac of the collider at 50 Hz repetition rate [1,2]. A conventional positron source uses only a single amorphous target. The CLIC source takes advantage of a novel hybrid target design consisting of a thin crystal target to enhance photon production via channelling and an amorphous target to convert the photons into positrons. In between a magnet is used to sweep out charged particles to reduce the peak power deposition on the production target [3]. In the Conceptual Design Report (CDR), a prove of principle approach was used to describe the design of the positron production chain for CLIC, estimating a positron yield of 0.39 e^+/e^- from the target to the entrance of the pre-damping ring [4,5]. The positron yield is defined as the number of positrons at a given place along the production chain per electron impinging onto the target. A study was launched to substantially improve the positron yield in this area to increase the margin of the positron target in terms of peak energy deposition and to

* Corresponding author at: Ankara University, Ankara, Turkey
E-mail address: cafer.bayar@cern.ch (C. Bayar).

http://dx.doi.org/10.1016/j.nima.2017.07.010
Received 14 March 2017; Received in revised form 17 May 2017; Accepted 7 July 2017
Available online 17 July 2017

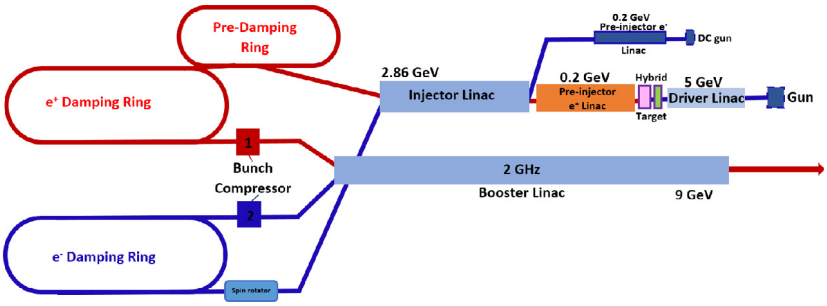

Fig. 1. Schematic layout of the CLIC injector complex consisting of an electron source, a positron source, a booster linac at 9 GeV, pre-damping and damping ring complex including a spin rotator and two bunch compressors.

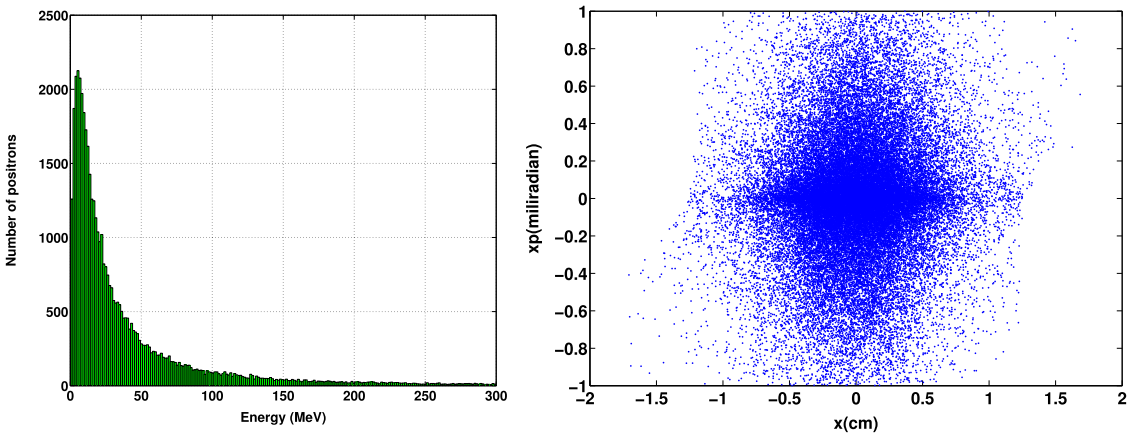

Fig. 2. Positron distribution after the target. The left figure shows the energy spectrum of positrons applying a cut at 300 MeV and the right figure shows the transverse phase space of positrons.

reduce the cost and energy consumption of the required electron driver linac. The CLIC positron source includes a hybrid target, an Adiabatic Matching Device (AMD), the pre-injector linac and the injector linac.

After the amorphous target, the conical magnetic field of the AMD focuses the positrons in order to be efficiently captured in the downstream accelerating structures. The longitudinal magnetic field of the AMD changes from 6 to 0.5 T in 20 cm. Two thirds of the positrons created in the target are already lost before entering the first accelerating structure. The CLIC positron target was optimised for a 5 GeV electron driver obtaining a yield of 8 e^+/e^-[6]. After the AMD, modelled using PARMELA [7], it was found that only 2.8 e^+/e^- survive due to the enormous energy spread and angular divergence of the generated positrons [8]. The aim of the study described in the following, is to preserve as many as possible of these precious positrons during acceleration and transport them up to the pre-damping ring. Intuitively, the positron-capture linac should increase the positron energy as fast as possible to reduce the divergence and the energy spread. However, it has been shown in the past that initial deceleration can lead to a more efficient capturing [9].

The CLIC positron source divides the acceleration into a pre-injector linac, which accelerates the positrons up to 200 MeV, and a final injector linac, which boosts the energy up to 2.86 GeV, which is the injection energy of the pre-damping rings. This separation comes from the fact that the injector linac is used both for electrons and positrons in the CLIC injector complex. The positrons are then injected into a pre-damping ring and a damping ring to reduce their emittance and finally accelerated to 9 GeV for transport into the main linac. The pre-damping ring has a limited transverse and longitudinal acceptance. Most critical for the positron beam is the energy acceptance window of 1.2%. The CLIC injector complex is shown schematically in Fig. 1.

In this paper, we describe the design and optimisation of the pre-injector linac and the injector linac with the objective to maximise the positron yield into the pre-damping ring acceptance.

2. The design of the CLIC pre-injector linac

The CLIC pre-injector linac has been optimised from the exit of the target up to an energy of the captured positrons of roughly 200 MeV. Starting point was the simulated positron distribution at the exit of the target from the previous study [6]. After production on the target with 5 GeV electrons, positrons have naturally large energy spread and emittance. The resulting positron distribution after the target is shown in Fig. 2. The average energy of the positrons is about 50 MeV at this stage. The initial design of the pre-injector linac, documented in the CDR, focused on capturing the positrons with energies up to roughly 100 MeV. The other natural cut on this enormous distribution was the transverse acceptance of the AMD and the accelerating structures, given mainly by their physical aperture.

An aperture of 20 mm radius has been chosen for the design of the 2 GHz accelerating structure as a compromise between obtainable gradient and power consumption. The model was based on a 1.5 m long $2\pi/3$ travelling wave structure with a gradient of up to 15 MV/m. For the simulations we assumed that the whole pre-injector linac is embedded into a solenoidal magnetic field of 0.5 T. The AMD reduces the beam divergence and concentrates a maximum of particles into the aperture of the first structure. The 6 T maximum field is believed to be feasible for such an aperture in a pulsed normal-conducting device. The length of the beam pulse is 176 ns. Both operation modes, acceleration and deceleration in the first rf structure, have been studied.

2.1. The accelerating mode in the pre-injector linac

In the accelerating mode, we placed the centre of the positron distribution on the crest of the accelerating field, and accelerated with a 15 MV/m gradient in each structure. The drift space between structures was chosen to be 20 cm. In this configuration the total length of the pre-injector linac is about 14 m, using 8 accelerating structures. At the end of

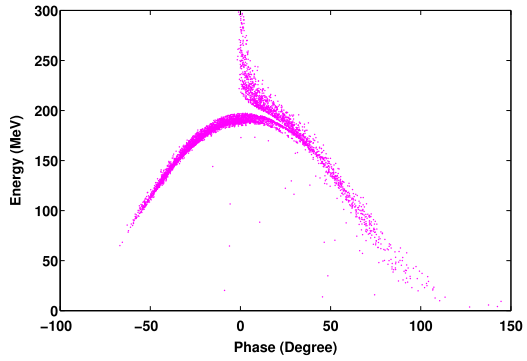

Fig. 3. Energy and phase distribution in the end of the pre-injector linac for the decelerating mode.

the linac the average particle energy reaches 200 MeV. The longitudinal phase space obtained can be seen in Fig. 8.

All the simulations of the pre-injector linac were performed using the particle tracking code PARMELA. At the end of the pre-injector linac, the simulation showed that the total positron yield, including all particles, is 0.89 e^+/e^-, meaning that only about 10% of the produced positrons are captured. Since we are interested in optimising the yield of positrons, which likely will end up within the acceptance of the pre-damping ring, we defined for the optimisation as a figure of merit an effective yield describing the particles which are in a ±20 degrees and ±50 MeV energy window. After simulations, the corresponding effective yield has been found to be around 0.5 e^+/e^- in the acceleration mode. These results are comparable with earlier studies on CLIC CDR [4,10].

2.2. The decelerating mode in the pre-injector linac

The decelerating mode was proposed firstly in 1979 by Aune and Miller [9]. The advantages of the deceleration have been tested experimentally and it has been shown that it can provide a better positron yield. In the CLIC CDR [1,4], the decelerating mode was applied in the pre-injector linac using a phase close to the maximum deceleration in the first structure. A modest gradient of 6 MV/m for the deceleration in the first structure was applied. As a starting point, we have verified the results of the CDR studies. After the first structure at 6 MV/m, a maximum acceleration of 15 MV/m was used with on crest acceleration along the pre-injector linac.

In Fig. 3, the longitudinal distribution of positrons in the decelerating mode is shown. Compared to the accelerating mode, more positrons are captured. The total yield is 0.93 e^+/e^- and the effective yield in a ±20 degrees and ±50 MeV energy window is around 0.48 e^+/e^-, agreeing well with the previous results documented in the CDR.

2.3. Optimisation of the pre-injector linac in the decelerating mode

For a better understanding the trapping of the positrons during deceleration and acceleration, the process was simulated in detail varying the phase of the accelerating fields over the full range of 360°. The result was that the phase range between maximum deceleration and the following zero-crossing is optimal for capturing the positrons with such an initial distribution. Here the fields provide eventually both focusing and acceleration. For our case a phase of 40° after maximum deceleration turned out to be optimum. The different phases used in the simulations are illustrated in Fig. 4. The positrons are first decelerated, but slip over into the accelerating phases already in the first structure.

Looking at the phase spectrum during this process independent of the phase initially chosen one can notice that particles get trapped into at least two adjacent rf buckets due to the large energy spread. By choosing the phase one can control the amount of particles trapped in either bucket. The accelerating mode collects most of its particles in the first rf bucket keeping them on crest, whereas the decelerating mode shuffles more particles in the following rf bucket. The optimum yield was found maximising the second peak of the phase distribution in the first structure and then accelerating this peak on crest in the rest of the linac, see Fig. 5.

The results have a better yield and, even more importantly, a better phase space distribution. A nice compact peak is obtained in the phase and energy distribution.

Fig. 6 shows the mean energy of positrons along the beam line in the optimised decelerating mode. The mean energy of positrons is about 50 MeV at the exit of the target and it is around 80 MeV after the AMD as seen Fig. 6, because low energy positrons are lost very quickly. In the first structure, the deceleration is applied in the optimum phase and therefore a longer beam line about 19 m in total is needed to get to 200 MeV.

Besides the phase in the first structure, another important parameter is the deceleration gradient. The deceleration gradient is scanned for different values in terms of positron yield. A high gradient of at least 12 MV/m is favoured for the deceleration mode (see Fig. 7). While the total yield is not affected dramatically, the higher gradient results in a narrower phase and energy spectrum.

Fig. 8 compares the longitudinal phase space at the end of the pre-injector linac for the accelerating mode and the optimised decelerating mode. It is clearly visible that accelerating on crest right away results in a large tail in the distribution while in the deceleration case it is possible to fold in a good fraction of the particles otherwise ending up in the tail. In this case the total yield is 1.09 e^+/e^- and the effective yield is around 0.98 e+/e- at the exit of the pre-injector linac showing that the main benefit is a better suited longitudinal phase space for acceptance into the damping ring. Therefore the optimised decelerating mode result in almost a factor two higher yield compared to the accelerating mode which has a yield of 0.5 e^+/e^-.

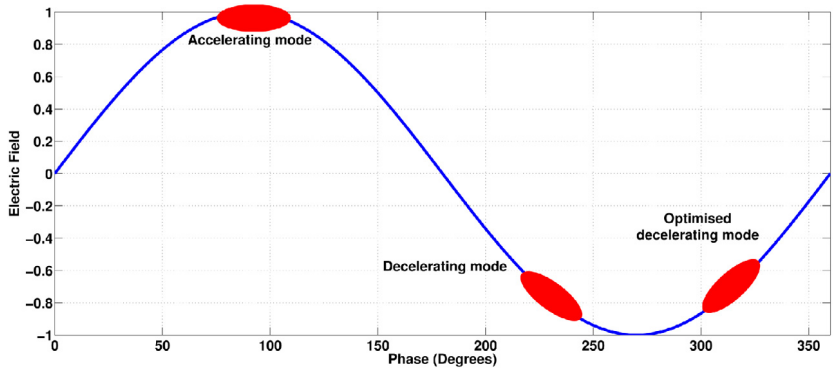

Fig. 4. A sketch of the electric field with "bunches" placed on the different phases for acceleration, deceleration (CDR) and optimised deceleration.

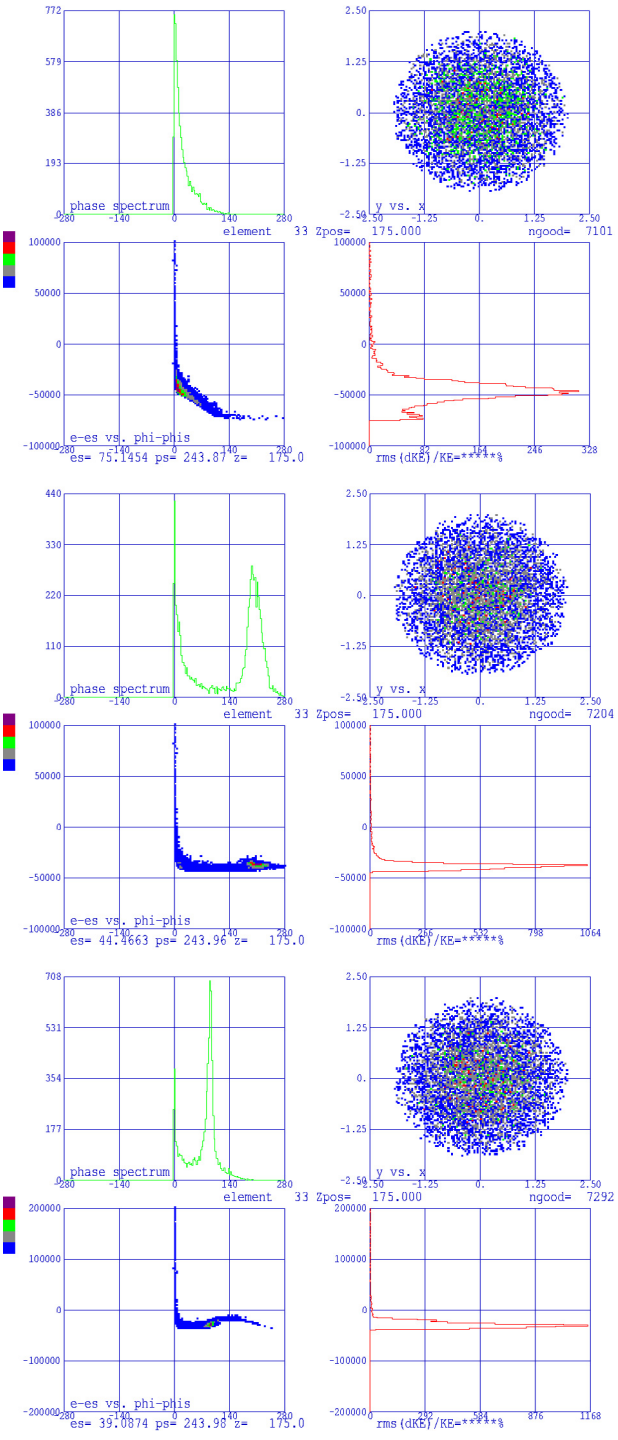

Fig. 5. Positron distributions for the different operation models, accelerating (upper), decelerating (middle) and optimised decelerating (bottom) at the exit of the first structure. The upper right plot is the transverse beam size in cm, the bottom left graph is the longitudinal phase space with its projection into phase in degrees (upper left) and energy in eV (bottom right) for each figure. All the phases are with respect to a reference particle defined in PARMELA.

3. The design of the CLIC injector linac

The CLIC injector linac is supposed to accelerate positron beams and electron beams simultaneously from 200 MeV after the pre-injector up to the damping ring energy of 2.86 GeV. Since the emittance of the positron beam is much larger compared to the electron beam the optics design is done for the positrons. First conceptual studies of the injector linac have been performed for the CLIC CDR [5,11–13]. The main strategy of the design was to transport the beam with as little loses as possible from the pre-injector linac to the pre-damping ring and if necessary optimise the longitudinal phase space to match the acceptance of the pre-damping ring.

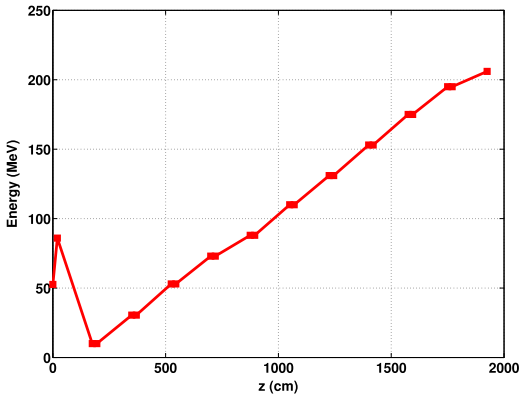

Fig. 6. Mean energy profile along the pre-injector linac in the optimised decelerating mode. The decelerating mode requires 3 additional accelerating structures to bring the energy up to 200 MeV.

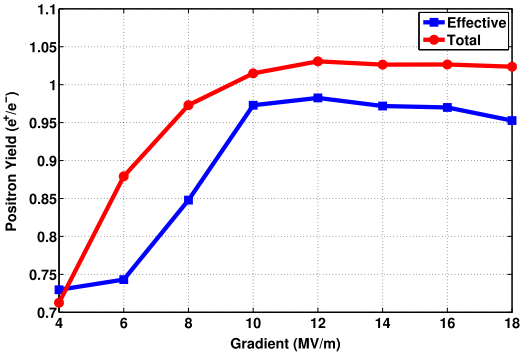

Fig. 7. Positron yield at the end of the pre-injector linac versus the gradient of the first structure.

The main limiting factor for the beam transport is the aperture of the linac due to the large transverse emittance of the positron beam. In the previous design studies mostly triplet lattices have been used followed by a bunch compressor in the end to rotate the phase space to maximise the yield into the damping ring longitudinal acceptance. In our new study several sections of FODO lattices are used along the whole linac and a rotation of the phase space is no longer required due to the optimisation in the pre-injector linac.

3.1. Optical design of the CLIC injector linac

The positron distribution obtained from PARMELA of the optimised pre-injector linac has been used at the entrance of the injector linac for the simulations. Since the beam is now fully relativistic we use MAD-X [14] for the lattice design and PLACET [15] for particle tracking. We use the same accelerating structure as in the pre-injector linac with a length of 1.5 m, a gradient of 15 MV/m and an iris radius of 20 mm. It is desired to transport most of the particles through the accelerator, therefore we want the 3σ beam size not to exceed the iris aperture.

The normalised emittance ($\varepsilon_{x/y}$) at the exit of the pre-injector linac is 9.6×10^{-3} rad m and the mean energy of the beam is 200 MeV. Using Eq. (1) we determine that the maximum beta function should be smaller than 1.8 m for an iris aperture (R_{iris}) of 20 mm at the beginning of the injector linac.

$$\beta_{\max} \leq \frac{R_{iris}^2}{9}\frac{\gamma}{\varepsilon_{x,y(norm)}}. \quad (1)$$

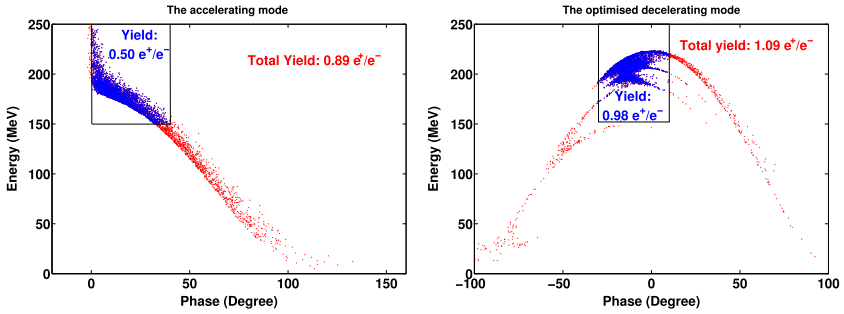

Fig. 8. Longitudinal phase space for the accelerating mode and the optimised decelerating mode.

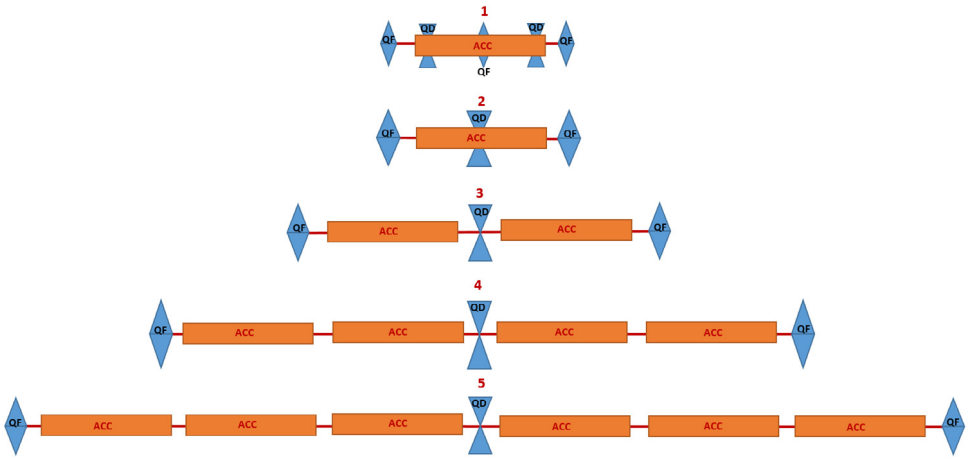

Fig. 9. Schematic layout of the five different sections in the FODO lattice along the CLIC injector linac. QF: focusing quadrupole, QD: defocusing quadrupole and ACC: accelerating structure.

Here, $\beta_{\max}$ is the largest value of the betatron function along the first accelerating structure and γ is Lorentz factor corresponding the minimum energy sector and $\epsilon_{x,y(norm)}$ is the normalised emittance. The injector linac needs therefore strong focusing at the entrance. For a FODO lattice the minimum beta-function depends on the strength of the quadrupoles and on the spacing between them. A phase advance of 90° is used for the design since for round beams we obtain the smallest maximum beta-function within the FODO cell [16]. For practical reasons, we limited the maximum field of the quadrupoles to 1.2 T and choose a quadrupole aperture R_Q of 0.1m. This choice of parameters allows us to use quite standard quadrupoles with an aperture large enough to go over a 2 GHz accelerating structure at the beginning of the injector linac. Using this logic, five different FODO sections have been designed with increasing spacing in-between quadrupoles such that the above limitations are respected.

In this way, for example, the first section of the injector linac (see sketch in Fig. 9 has been designed with the following parameters: the length of the quadrupole is 0.4 m and the drift space between quadrupoles is 0.15 m. We obtain $\beta_x = 1.716$ m, $\beta_y = 0.346$ m in the focusing quadrupoles.

The acceleration along the beam line makes it possible to have a larger beta-function due to the reduction of the geometric emittance. The design profits from that by increasing the distance between quadrupoles. From the third section on quadrupoles can be placed in between accelerating structures allowing in principle for smaller aperture magnets. Using several sections reduces the number of quadrupoles needed without compromising on the beam transport. The parameters of all sections can be found in Table 1. The beta-functions along the linac in the five different sections are shown in Fig. 10 and the corresponding beam envelopes in Fig. 11.

A total of 19 quadrupoles are used for matching between the different sections. The simulations for the lattice design have been

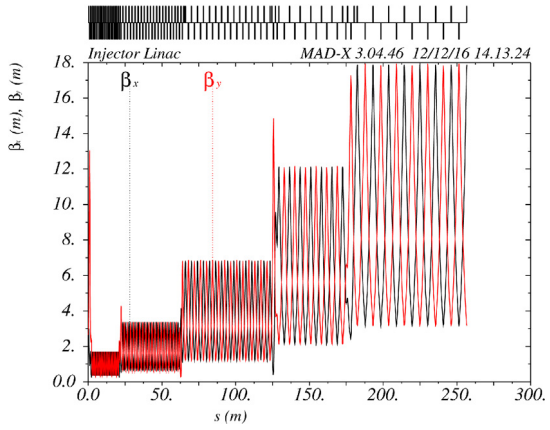

Fig. 10. Horizontal and vertical beta functions along the CLIC injector linac.

done initially with MAD-X without considering acceleration to avoid the problem of having quadrupoles at the same place as accelerating structures. For the plot of the beam sizes the increase in energy has been taken into account showing that the aperture of 20 mm can house a 3σ beam with the exception of the first matching section. This design allows to reduce the number of quadrupoles used to 146 compared to 192 in the CDR.

3.2. Tracking simulation of the CLIC injector linac

After finishing the optical design of the CLIC injector linac, the tracking simulations have been performed using the particle tracking

Table 1
Parameters of the five different sections in the FODO lattice along the CLIC injector linac.

Sections	Q_{length} (m)	K(m^{-2})	β_{max} (m)	$Cell_{length}$ (m)	E_{ini} (GeV)	E_{out} (GeV)	$Q_{numbers}$
1	0.4	9.00	1.7160	1.10	0.2065	0.3865	33
2	0.4	3.95	3.3860	2.08	0.3865	0.7915	37
3	0.4	1.85	6.8252	4.10	0.7915	1.4215	29
4	0.4	1.02	12.1250	7.20	1.4215	2.0515	15
5	0.4	0.68	17.8860	10.60	2.0515	2.8615	13

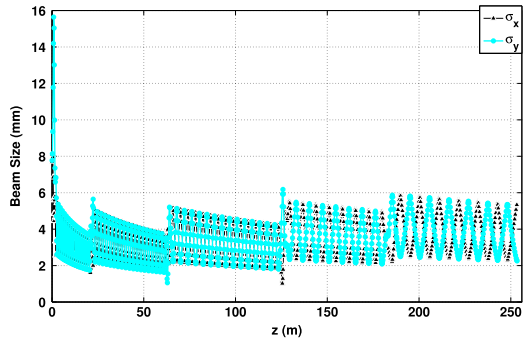

Fig. 11. Positron beam horizontal and vertical envelopes along the CLIC injector linac.

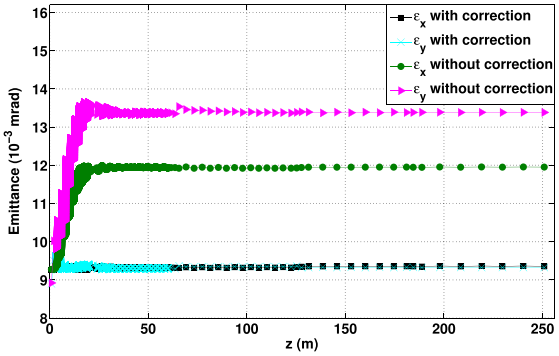

Fig. 12. Emittance growth along the CLIC injector linac.

code PLACET. The definition of the quadrupoles around RF structures as used in the first and second sections is not foreseen in PLACET. Therefore, we have used the following approach: a quadrupole with a length of 0.4 m has been split in 400 zero-length slices (in thin-lens approximation) with thick RF structures, 1-mm long, between two consecutive quadrupole kicks to impart the appropriate acceleration.

After verifying the beam line without acceleration, the optical functions were checked with acceleration using PLACET for positrons coming from the pre-injector linac. PLACET calculates the Twiss parameters from the particle distribution and takes into account the focusing effect of the accelerating structures. The realistic modelling of the accelerating and the overlapped focusing fields resulted in a mismatch of the betatron functions compared with respect to the energy-independent MAD-X design.

Fig. 12 shows the emittance evaluated along the beam line. A significant emittance growth due to the very high energy spread of the positron beam, in particular at the beginning of the linac, is visible. This emittance growth depends on the beta-function therefore we get an asymmetry between the vertical and horizontal plane. PLACET allowed us to optimise the emittance growth by slightly varying the quadrupole strength along the linac. The emittance growth can be mitigated by this optimisation adapting mainly the quadrupole strengths in the first matching section (see Fig. 12)

After correction of the emittance growth, Fig. 13 shows the phase space obtained for positrons at the exit of the beam line. The important

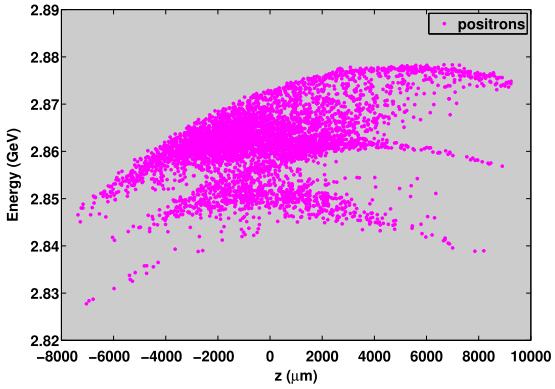

Fig. 13. Longitudinal phase space at the exit of the CLIC injector linac.

result is that the positron yield amounts to 0.97 e^+/e^- about a factor 2.5 higher than the 0.39 e^+/e^- which were previously estimated and published in the CDR. Another important result is that all particles are inside the acceptance window of the pre-damping ring without a need of phase space rotation. To transport basically all the beam without losses through the injector linac, it was necessary to increase the aperture of the beam pipe in the quadrupoles to 4 cm in particular in the first matching section. An aperture of 2 cm all long the beam line would have resulted in a 10% loss of positrons.

4. Conclusion

The accelerating and decelerating positron capturing modes have been studied for the CLIC positron source. The decelerating mode has been optimised to capture more positrons at the exit of the pre-injector linac. The optimum gradient and phase have been determined for the first structure in the decelerating mode. This new optimisation results in a factor 2.5 increase of the positron yield delivered into the acceptance of the pre-damping ring. This allows to reduce the beam current of the electron driver linac impinging onto the target accordingly, resulting in significant cost savings and a larger margin for the peak energy deposition into the target. In consequence a single target can be used as well for the first stage of CLIC at 380 GeV. In the original study for the CDR, it was assumed two target in parallel would be needed to insure the higher beam current at this stage. The effective yield after the pre-injector linac amounts to 0.98 e^+/e^- and after the injector linac we have 0.97 e^+/e^- within the acceptance of the pre-damping ring.

Further improvements are still possible. During the simulations it became clear that increasing the aperture of the AMD and the accelerating structure would directly increase the yield as well increasing the strength of the solenoidal field around the pre-injector linac. However it remains to be seen if such changes are technically viable.

Acknowledgement

The authors are grateful to Olivier Dadoun for providing the positron distribution at the exit of amorphous target for this study.

References

[1] M. Aichler, P. Burrows, M. Draper, T. Garvey, P. Lebrun, K. Peach, N. Phinney, H. Schmickler, D. Schulte, N. Toge (Eds.), A Multi-TeV Linear Collider Base on CLIC Technology: CLIC Conceptual Design Report, CERN-2012-007, CERN, Geneva, 2012, pp. 99–107.

[2] P.N. Burrows, P. Lebrun, L. Linsen, D. Schulte, E. Sicking, S. Stapnes, M.A. Thomson (Eds.), Updated Baseline for a Staged Compact Linear Collider, CERN-2016-004 CERN, Geneva, 2016.

[3] L. Rinolfi, R. Chehab, O. Dadoun, T. Kamitani, V. Strakhovenko, A. Variola, Brilliant Positron Sources for CLIC and other Collider Projects, CLIC-Note-985, CERN, Geneva, 2013.

[4] F. Poirier, L. Rinolfi, A. Vivoli, O. Dadoun, P. Lepercq, A. Variola, Dynamics on the Positron Capture and Accelerating Section of CLIC, CLIC-Note-877, CERN, Geneva, 2011.

[5] A. Vivoli, I. Chaikovska, R. Chehab, O. Dadoun, P. Lepercq, F. Poirier, L. Rinolfi, V. Strakhovenko, A. Variola, The CLIC Positron Capture and Acceleration in the Injector Linac, CLIC-Note-819, CERN, Geneva, 2010.

[6] O. Dadoun, I. Chaikovska, P. Lepercq, F. Poirier, A. Variola, L. Rinolfi, A. Vivoli, R. Chehab, V. Strakhovenko, C. Xu, The baseline positron production and capture scheme for CLIC, in: Proceedings of IPAC10, Kyoto, Japan, 2010.

[7] L. Young, PARMELA Reference Manual, LA-UR-96-1835, Los Alamos national Laboratory, 2005.

[8] C. Bayar, S. Doebert, A.K. Ciftci, Beam dynamics simulation and optimization of the CLIC positron source and capture linac, AIP Conf. Proc. 1722 (2016) 070001. http://dx.doi.org/10.1063/1.4944155.

[9] B. Aune, R.H. Miller, New Method for Positron Production at SLAC, SLAC-PUB-2393, USA, 1979.

[10] F. Poirier, Positron Capture Section Studies for CLIC, Presentation of POSIPOL2011, IHEP, Beijing, China, 2011.

[11] A. Ferrari, L. Rinolfi, F. Tecker, Particle Tracking in the CLIC Main Beam Injecor Linac, CLIC-Note-665, CERN, Geneva, 2006.

[12] A. Ferrari, A. Latina, L. Rinolfi, Injector and Booster Linacs with the 2007 Beam Parameters, CLIC-Note-737, CERN, Geneva, 2008.

[13] A. Ferrari, L. Rinolfi, F. Tecker, Design Study of the CLIC Main Beam Injector Linac, CLIC-Note-626, CERN, Geneva, 2005.

[14] MAD-X, http://madx.web.cern.ch/madx/.

[15] PLACET, https://clicsw.web.cern.ch/clicsw/.

[16] H. Wiedemann, Particle Accelerator Physics, third ed., Springer, 2007 (Chapter 7).